Bettahar, Houari; Valisalmi, Teemu; Linder, Markus; Zhou, Quan

Robotic Fiber Fabrication based on Solidification Force Control

Published in:
Proceedings of MARSS 2022 - 5th International Conference on Manipulation, Automation, and Robotics at Small Scales

DOI:
10.1109/MARSS55884.2022.9870490

Published: 01/01/2022

Document Version
Peer reviewed version

Robotic Fiber Fabrication based on Solidification Force Control

Houari Bettahar, Teemu Välisalmi, Markus Linder, Quan Zhou, *Member, IEEE*

***Abstract*— In this paper, we propose a robotic fiber fabrication method based on solidification force control to achieve highly repeatable mechanical properties of fibers. Dextran material is used as the specimen in the experiments. It has been chosen because of its similar rheological behavior to silk protein at high mass concentrations. However, the viscosity of dextran material is very low at its liquid phase, so force control during fabrication is challenging. Here, we propose a novel approach that controls the mechanical properties of fiber by controlling the solidification force. We employ impedance control with force tracking to control the solidification force to carry out the threading experiments and examine the benefits of the proposed approach. The repeatability of the mechanical properties of the fabricated fibers has been studied and compared using three scenarios a) fiber fabrication without solidification force control, abbreviated as FFNC, b) fiber fabrication with solidification force control after 60 seconds of solidification from the beginning of the solidification force detection abbreviated as FFWC, and c) fiber fabrication with solidification force control immediately after the detection of the solidification force, abbreviated as FFSC. The experimental results show that fibers fabricated using FFSC scenario have the highest repeatability based on the coefficient of variation of properties of the fabricated fibers, where the obtained coefficient of variation of the toughness, stiffness, elongation, and strength are 12.8%, 13.6%, 14.8%, 12.7% respectively. The experimental results also showed that fibers' mechanical properties toughness, stiffness, elongation, and strength have a negative correlation with the fabrication pulling velocity.**

***Index Terms*—robotics and automation, artificial fiber threading, bio-mimicking, impedance control, force control**

I. Introduction

Fiber-shaped materials are very important in making various functional three-dimensional (3D) objects. Fibers are long, thin, and soft, and these properties help higher-order assemblies such as nanoscale materials [1] [2], clothes [3], and architectures [4] by folding, bundling, reeling, and weaving fibers. For example, hydrogel microfiber structures have been used to recapitulate biological tissues' architecture and functionality at the microscale [5] [6]. Hybrid polymer hydrogel fibers have also been used in soft biomimetic actuators and sensors with shape-changing capabilities in soft macro- and microrobotics [7] [8], as well as flexible microfiber strain sensor with a beads-on-a-string structure [9].

Despite all the advances in abundant fiber applications, a little study can be found in fiber fabrication beyond basic gel extrusion and threading. The gel-like matter is a mixture of liquids, gases, and solids with multiple surfaces that exhibit nonlinear responses, making the material highly deformable, highly viscose, and thermally sensitive, and its phase frequently changes. Because of these characteristics, manipulating gel-like matter is extremely difficult, so a detailed understanding and correct definition of its properties is essential. The threading of silk proteins and a variety of polymer materials to generate artificial threads has been the subject of scientific research. A variety of techniques have been used, e.g., wet-spinning [10], dry-spinning [11], electrospinning [12], microfluidic spinning [13], and direct writing [14]. So far, their mechanical properties, especially the strength and toughness of the produced artificial fibers can reach only about one-fifth of that of natural fibers such as spider silk fiber [15]. One of the reasons is that the fabrication process is either manual or based on open-loop regulation, e.g. velocity or position regulation.

Many natural species, on the other hand, can manipulate silk material with their bodily structures. Silk spinning in spiders and silkworms are prime examples [16] [17]. Using spinnerets and claws, a spider, for example, may perform a sophisticated pultrusion. By changing the interaction (pulling) forces, a spider can tune the mechanical properties of silk during threading, allowing protein dope to be continually converted into fibers with exceptional mechanical properties [15]. The produced fibers are one of the strongest and toughest biological materials, outperforming most synthetic polymers and even some metal alloys. In our recent work [18], a robotic gel fiber fabrication method based on impedance control with force tracking was proposed to control the pulling and solidification forces. The proposed method produced fibers with higher mechanical properties compared with fibers fabricated using open-loop pulling velocity regulation. To validate the proposed method, a commercial fast-curing contact adhesive (Pattex), which is a solvent-based polychloroprene rubber, was used to generate artificial fibers. However, this fast-curing contact adhesive (Pattex) has a very different rheological behavior than natural silk.

In this paper, we propose a robotic fiber fabrication method based on solidification force control to achieve highly repeatable mechanical properties of fibers. Dextran material is used as the specimen in the experiments. It has been chosen because of its similar rheological behavior to silk protein at high mass concentrations. However, the viscosity of dextran material is very low at its liquid phase, so force control during fabrication is challenging. Here, we propose a novel approach that controls the mechanical properties of fiber by controlling the solidification force. We employ impedance control with force tracking developed in [18] to control the solidification force. The repeatability of the mechanical properties of the fabricated fibers has been studied and compared using three scenarios a) fiber fabrication without solidification force

*Research supported by Academy of Finland Project 317018. The authors are with the Department of Electrical Engineering and Automation, School of Electrical Engineering, Aalto University, 02150 Espoo, Finland. Email address: houari.bettahar@aalto.fi, teemu.valisalmi@aalto.fi, markus.linder@aalto.fi, corresponding author: quan.zhou@aalto.fi.

control, abbreviated as FFNC, b) fiber fabrication with solidification force control after 60 seconds of solidification from the beginning of the solidification force detection abbreviated as FFWC, and c) fiber fabrication with solidification force control immediately after the detection of the solidification force, abbreviated as FFSC.

The paper is organized as follows. Section II describes the experimental setup. Section III introduces the experimental protocol and impedance control with force tracking used to control the solidification force. Section IV reports and discusses the experimental results. Finally, section V concludes the paper.

II. Experimental Setup

The experimental setup for Dextran fiber fabrication is shown in **Fig. 1**. Dextran dispenser is installed at the lower part of the setup, mounted on a motorized precision positioner (Physik Instrumente, model M-404.4PD). For pulling experiments, a capillary needle is mounted on a fixed force sensor (LCM Systems, model LCM UF1) to sense the pulling force after contacting the Dextran at the tube of the dispenser. The force sensor (LCM Systems, model LCM UF1) is based on strain gauges, which return a signal proportional to the mechanical force applied for the gel pulling. It has a resolution of 0.05 g and an estimated stiffness of $8 \times 10^3\ N/m$. The motorized precision positioner is controlled via a controller (Physik Instrumente, model C-884.4CD). The measurement of the force sensor is acquired using a data acquisition (DAQ) board (National Instrument, model PCIe-6363). The whole setup is constructed on a vibration isolation table and controlled using Matlab/Simulink.

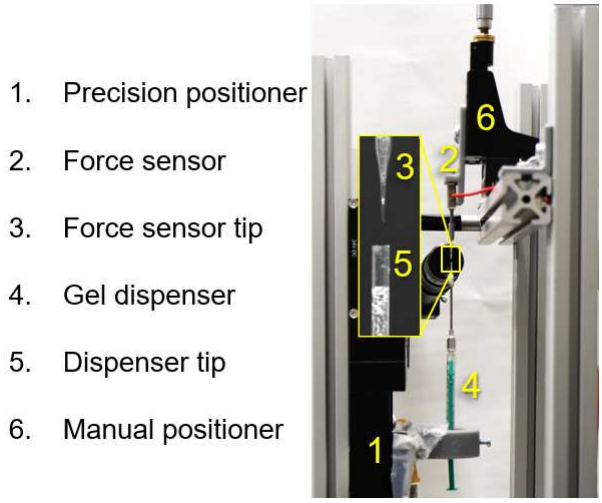

Fig. 1. The experimental setup for robotic fiber fabrication. The force sensor is fixed on a frame, and the Dextran dispenser is mounted on a motorized precision stage.

Dextran is a polymerized Glucose mixed with water, used as the gel specimen in the experiments. Dextran is chosen because of its similar rheological behavior to silk protein at high mass concentrations. Dextran is also easy to produce, can be stored by flash freezing in a freezer, and thawed without structural changes.

III. Materials and Methods

A. Fiber fabrication protocol

The proposed fiber fabrication procedure is shown in **Fig. 2**, including the dispensing phase, and both the Dextran fiber fabrication and characterization phases. In the dispensing phase, the force sensor tip is inserted into the dispenser tube until it contacts the Dextran material. In the fiber fabrication phase, the Dextran is pulled using the manipulator for a given distance (referred to as fabrication pulling, and the force is referred to as fabrication force). Then, the manipulator is kept steady for a given time while the fiber is solidifying (referred to as solidification force). In the fiber characterization phase, the fiber is pulled again (referred to as characterization pulling, and the force is referred to as characterization force) to investigate the mechanical properties of the fabricated fibers using the force-extension curve after the fiber fabrication phase.

Dextran fiber fabrication is the process of pulling the Dextran material to transform it from a liquid to semi-solid and consequently producing a fiber. During the solidification, the chemical and molecular structure changes continuously, which affects the mechanical properties of the fiber and its

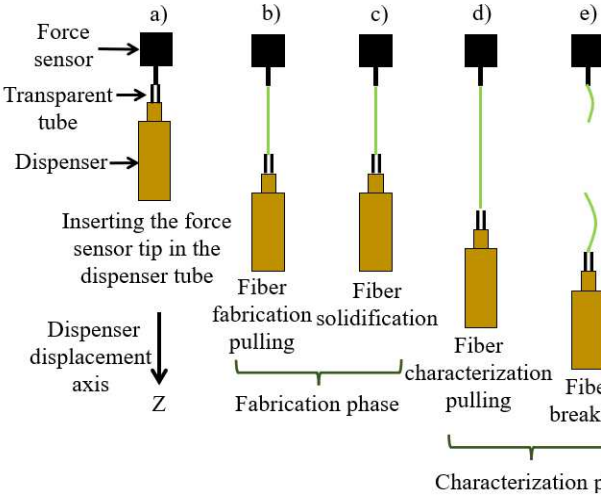

Fig. 2. The fiber threading experimental protocol. a) inserting the force sensor tip in the dispenser tube until it contacts the Dextran material; b) the dispenser moves away from the force sensor pulling the Dextran into a fiber until certain criteria are satisfied, e.g., in displacement or force; c) the system stalls for a certain amount of time to allow the fiber to solidify; d) the fiber is pulled further until e) the fiber breaks.

repeatability. Controlling the solidification force or tension force may increase the repeatability and control of the mechanical properties of the fibers. For this purpose, the next section will present the control approach used to control the solidification force during the fiber fabrication.

B. Fiber fabrication control

To control the fiber fabrication process, we employed the impedance control with force tracking developed in [18]. The objective, as introduced in [26], is to provide a desired user-specified dynamical relationship, referred to as, target impedance between the manipulator (consisting of the precision positioner and the dispenser) position z and the solidification force f_D. Typically, the target impedance is selected as a linear second-order system, so that the dynamical

relationship between the fabrication force f_D and the manipulator position z can be controlled by a mass-spring-damper system.

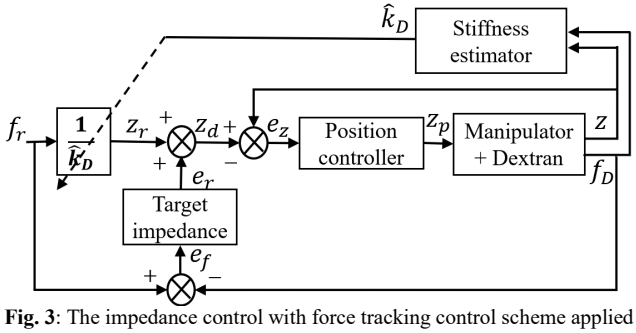

Fig. 3: The impedance control with force tracking control scheme applied on fiber threading during the fabrication process.

During the solidification of the fiber, the stiffness, damping, and mass of the Dextran change continuously. Therefore, all three parameters are variables with respect to time. The force applied by the manipulator on the Dextran is given by:

$$m_D(t)\ddot{z} + b_D(t)\dot{z} + k_D(t)z = f_D \quad (1)$$

where $m_D(t)$, $b_D(t)$ and $k_D(t)$ are respectively the mass, damping, and stiffness of the Dextran. z is the current position of the manipulator (tip of the dispenser), z_p is the output of the block "Position controller" (see **Fig. 3**), f_D is the force applied by the manipulator to the Dextran once contact between both is established. The f_D is the pulling force to be controlled based on impedance control.

A common mathematical description of the target impedance is given by (2), where M, B, and K are respectively the desired mass, damping, and stiffness of the target impedance, z_r is the reference position, f_r is the reference pulling force and e_f is the pulling force error.

$$M(\ddot{z} - \ddot{z}_r) + B(\dot{z} - \dot{z}_r) + K(z - z_r) = f_r - f_g = e_f \quad (2)$$

The position controller is implemented using the proportional-integral-derivative (PID) controller. Thus, the control law can be expressed as

$$z_p = k_p e_z + k_i \int e_z + k_v \dot{e}_z \quad (3)$$

where k_p, k_i, and k_v are the PID controller gains, where $e_z = z_d - z$, represents the position error between the desired generated position and the current position.

The steady-state pulling force error is given as derived in [18]:

$$e_f^{ss} = k_{eq}\left[\frac{f_r}{k_D(t)} + e_z - z_r\right] \quad (4)$$

where $k_{eq} = \frac{K k_D(t)}{K + k_D(t)}$ is the equivalent stiffness of the target impedance and the Dextran. The equation (4) means that if the control law of the position controller is used to reach a zero steady-state position error ($e_z \to 0$) and the reference position is selected precisely, then the steady-state force error will tend towards zero ($e_f^{ss} \to 0$).

However, the stiffness of the Dextran changes continuously during fiber pulling. An online estimation method is used to estimate the stiffness $k_D(t)$ during the whole threading process [18]. The Dextran stiffness is then estimated using the static part of the equation (1):

$$\hat{k}_D = \frac{f_D}{z} \; if \; z \succ 0 \quad (5)$$

Note that neglecting the dynamic part of equation (1) could change the desired dynamic of the system but it will not influence the steady-state part. The complete impedance control with the force tracking scheme used in this work is shown in **Fig. 3**.

In the experiments, the impedance control with the force tracking scheme presented in **Fig. 3** is implemented with a sampling frequency of 100 Hz without any knowledge of the stiffness of the Dextran before pulling. The control scheme was evaluated using the experimental setup presented in section II. The PID parameters of the position controller and the target impedance in **Fig. 3** have been tuned based on the trial-error method to achieve the desired force performances (time response, accuracy, and overshoot cancelation).

As shown in **Fig. 4,** during the dispensing and fiber fabrication pulling phases a) and b) (also see Fig. 2), the force is not detectable, because Dextran material has very low viscosity, However, during solidification, when the manipulator stalls for a given amount of time, the solidification force can be detected. The estimation of the stiffness then begins, and the impedance controller can track the force reference set to 5 mN with a response time of 6 s without overshoot, with a force tracking error of 0.007 mN (0.14%) and a position error of 0.0859 mm (0.29%). And the stiffness of the Dextran fiber is estimated continuously during control to be around 0.0835 N/m average.

In the next section, fiber fabrication with and without force control is studied.

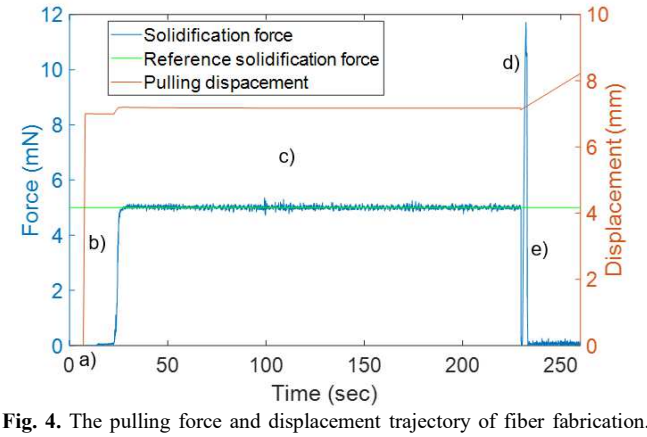

Fig. 4. The pulling force and displacement trajectory of fiber fabrication. experiment. During a) and b) (see Fig. 3), the force is not detectable, during solidification c) the system stalls for a certain amount of time to allow the fiber to solidify until the force starts to be detected, simultaneously the impedance controller is enabled to let the solidification force tracks the force reference; d) the fiber is pulled further until e) the fiber breaks.

IV. FIBER FABRICATION BASED ON SOLIDIFICATION FORCE CONTROL

All the experiments have been done under constant environmental conditions: temperature and relative humidity of 24 °C and a 63% respectively.

In this section, we investigate the impact of solidification force control using impedance control with force tracking [18], We use an experimental protocol as shown in **Fig. 2** to conduct experiments and characterize the mechanical properties of the fabricated fibers, and investigate the repeatability of the experiments. To judge the impact, we compared the repeatability results from fiber fabrication without solidification force control, abbreviated as FFNC; fiber fabrication with solidification force control 60 sec after the first detection of the solidification force, abbreviated as FFWC; and fiber fabrication with solidification force control immediately after the detection of the solidification force, abbreviated as FFSC. In the three cases, the pulling velocity is constant and equal to 50 mm/s.

After threading or the fabrication process in **Fig. 2**, the fabricated fiber is characterized using tensile testing, where the force-extension curve can be obtained. Force-extension curves can reveal key mechanical properties of fiber, e.g., toughness, stiffness, elongation, and strength. Toughness is the most remarkable property of biological materials. It is the capability of a material to consume the energy and gets deformed without breaking up. The stiffness of the material affects the degree it deflects under a load, and the strength is the property of a material that opposes the deformation or breakdown of material in the presence of load forces. The elongation-to-break is the deformation of a sample when it breaks.

To compare the results, we first studied the repeatability of the mechanical properties using the FFNC and FFWC scenarios. Five fibers are fabricated and characterized for each scenario following the experimental protocol in **Fig. 2**. The obtained force profile with respect to time for fiber fabrication and characterization phases are shown in **Fig. 5.a** and **Fig. 5.c** respectively**.** The corresponding characterization force-extension curves are shown in **Fig. 5.b** and **Fig. 5.d** respectively. The mean, standard deviation (SD), and coefficient of variation (CV) of the mechanical properties, toughness, stiffness, elongation, and strength are estimated as shown in Tables 1 and 2 respectively.

To investigate the repeatability of the mechanical properties of FFSC scenario, five fibers are fabricated and characterized. The obtained force profile with respect to time for fiber fabrication and characterization phases is shown in **Fig. 5.e,** and the corresponding characterization force-extension curves are shown in **Fig. 5.f**. The mean, standard deviation (SD), and coefficient of variation (CV) of the mechanical properties, toughness, stiffness, elongation, and strength are estimated as shown in Table 3.

We can notice that the repeatability of the mechanical properties using the proposed FFSC scenario is the highest, it has the lowest CV of the four mechanical properties, toughness, stiffness, elongation, and strength as **Fig. 6** and Tables 1,2 and 3. We attribute the inferior repeatability of the FFNC scenario to the uncontrolled solidification dynamics and steady-state solidification force, and the FFWC scenario to the uncontrolled solidification dynamics.

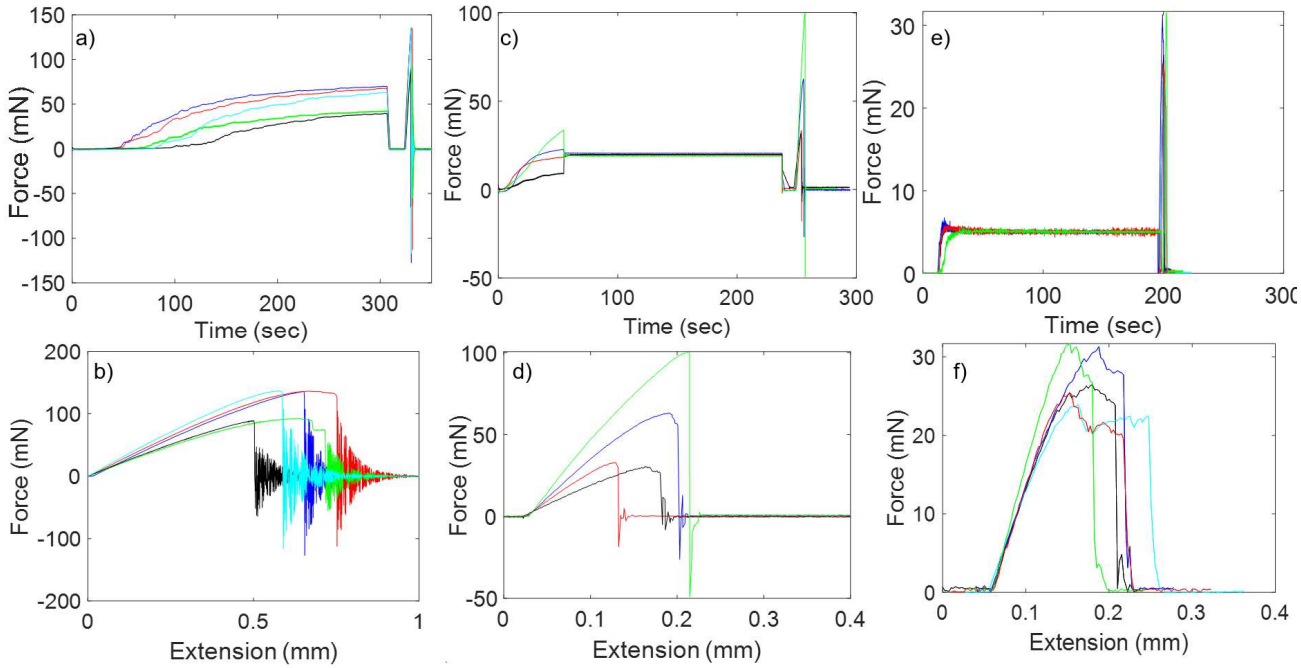

Fig.5: a) Force profile with respect to time for fiber fabrication and characterization phases for FFNC scenario, b) Force-extension curve after characterization FFNC scenario c) Force profile with respect to time for fiber fabrication and characterization phases for FFWC scenario, d) Force-extension curve after characterization FFWC scenario, e) Force profile with respect to time for fiber fabrication and characterization phases for FFSC scenario, f) Force-extension curve after characterization FFSC scenario.

TABLE 1: TOUGHNESS, STIFFNESS, ELONGATION, AND STRENGTH, FOR FFNC SCENARIO.

	Toughness ($10^{-6} \cdot$ J)	Stiffness (N/m)	Elongation (mm)	Strength (mN)
Mean	0.89	227.53	0.99	118.33
SD	0.29	31.29	0.42	24.99
CV	0.32	0.137	0.42	0.21

TABLE 2: TOUGHNESS, STIFFNESS, ELONGATION, AND STRENGTH FOR FFWC SCENARIO.

	Toughness ($10^{-6} \cdot$ J)	Stiffness (N/m)	Elongation (mm)	Strength (mN)
Mean	5.49	411.60	0.1613	56.79
SD	3.90	158.23	0.033	32.90
CV	0.71	0.38	0.20	0.57

TABLE 3: TOUGHNESS, STIFFNESS, ELONGATION, AND STRENGTH, FOR FFSC SCENARIO.

	Toughness ($10^{-6} \cdot$ J)	Stiffness (N/m)	Elongation (mm)	Strength (mN)
Mean	3.01	312.51	0.1818	27.76
SD	0.39	42.67	0.027	3.52
CV	0.128	0.136	0.148	0.127

To study the influence of the pulling velocity on the mechanical properties of the fabricated fibers using the proposed FFSC scenario, we applied four different pulling velocities 10, 15, 20, and 25 mm/s. The obtained force-extension curves **Fig. 7.a**. The mechanical properties of the fabricated fibers, in terms of toughness, stiffness, elongation, and strength corresponding to the four different pulling velocities are compared using bar diagrams as shown in **Fig. 7.b**. We can notice that the toughness, stiffness, elongation, and strength have a negative correlation with respect to the pulling velocity.

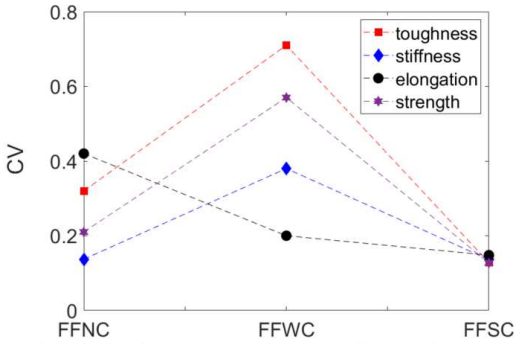

Fig.6: The obtained CV of toughness, stiffness, elongation, and strength for FFNC, FFWC, and FFSC scenarios.

V. CONCLUSION

Fiber-shaped materials are very important in making various functional three-dimensional (3D) objects. Fibers are long, thin, and soft, and these properties help higher-order assemblies such as nanoscale materials, clothes, architectures, etc. On the other hand, spiders, for example, can do a sophisticated pultrusion process. Their produced fibers outperform most synthetic polymers and even some metal alloys. To mimic and understand the spider threading process, a robotic fiber fabrication method based on solidification force control was designed to achieve highly repeatable mechanical properties of fibers. We employed impedance control with force tracking to control the solidification force to carry out fiber fabrication experiments. The repeatability of the mechanical properties of the fabricated fibers has been studied and compared using three scenarios a) fiber fabrication without solidification force control, abbreviated as FFNC, b) fiber fabrication with solidification force control after 60 seconds of solidification from the beginning of the solidification force detection abbreviated as FFWC, and c) fiber fabrication with solidification force control immediately after the detection of the solidification force, abbreviated as FFSC. The experimental results show that fibers fabricated using FFSC scenario have the highest repeatability based on the coefficient of variation of properties of the fabricated fibers, where the obtained coefficient of variation of the toughness, stiffness, elongation, and strength are 12.8%, 13.6%, 14.8%, 12.7%

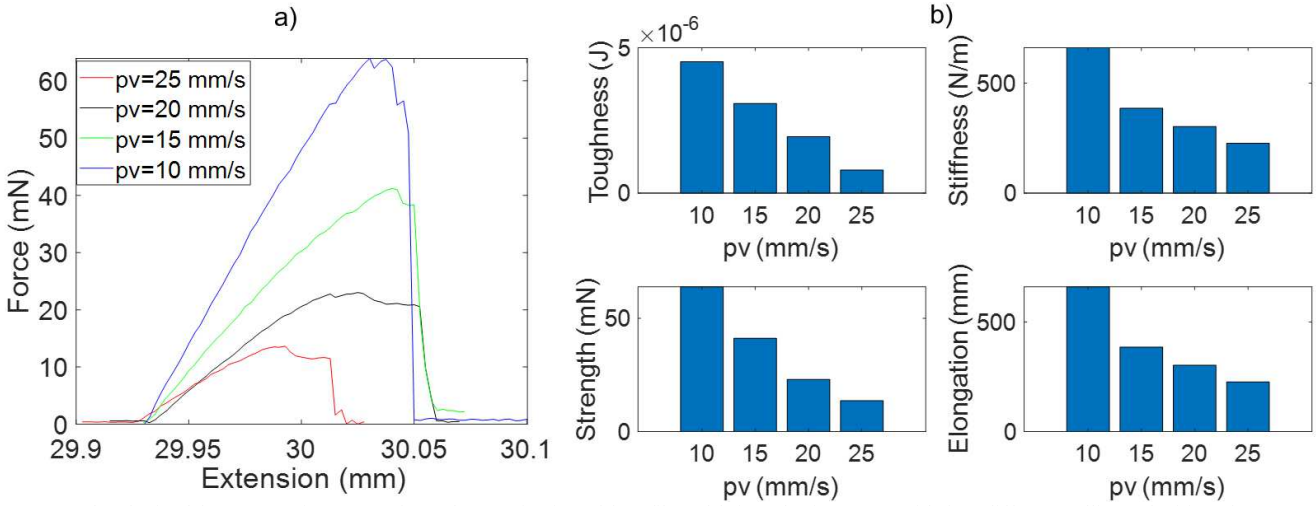

Fig.7: a) The obtained force-extension curves from characterization of four fibers fabricated using FFSC with four different pulling velocities of 10, 15, 20, and 25 mm/s.. g), b) The corresponding obtained mechanical properties: toughness, stiffness, elongation, and strength, for the four different pulling velocities of 10, 15, 20, and 25 mm/s.

respectively. The proposed based on FFSC scenario has also been used to study the influence of the fabrication pulling velocity on the mechanical properties of the fibers. The influence of the fabrication pulling velocity has been studied, showing that the mechanical properties toughness, stiffness, elongation, and strength have a negative correlation with the fabrication pulling velocity.

ACKNOWLEDGMENT

This work has been supported by the project 317018 AI spider silk threading (ASSET) in the AIPSE program of the Academy of Finland.

REFERENCES

[1] P. W. K. Rothemund, "Folding DNA to create nanoscale shapes and patterns," *Nat. 2006 4407082*, vol. 440, no. 7082, pp. 297–302, Mar. 2006, doi: 10.1038/nature04586.

[2] Y. Dzenis, "Spinning continuous fibers for nanotechnology," *Science (80-.).*, vol. 304, no. 5679, pp. 1917–1919, Jun. 2004, doi: 10.1126/SCIENCE.1099074/ASSET/3CD9D3AA-3492-49C7-B340-C72B525308FA/ASSETS/SCIENCE.1099074.FP.PNG.

[3] A. P. Mouritz, M. K. Bannister, P. J. Falzon, and K. H. Leong, "Review of applications for advanced three-dimensional fibre textile composites," *Compos. Part A Appl. Sci. Manuf.*, vol. 30, no. 12, pp. 1445–1461, Dec. 1999, doi: 10.1016/S1359-835X(99)00034-2.

[4] B. Quinn, "Textiles in architecture," *Archit. Des.*, vol. 76, no. 6, pp. 22–26, 2006, doi: 10.1002/AD.348.

[5] H. Onoe *et al.*, "Metre-long cell-laden microfibres exhibit tissue morphologies and functions," *Nat. Mater. 2013 126*, vol. 12, no. 6, pp. 584–590, Mar. 2013, doi: 10.1038/nmat3606.

[6] C. F. Guimarães, L. Gasperini, A. P. Marques, and R. L. Reis, "3D flow-focusing microfluidic biofabrication: One-chip-fits-all hydrogel fiber architectures," *Appl. Mater. Today*, vol. 23, p. 101013, Jun. 2021, doi: 10.1016/J.APMT.2021.101013.

[7] D. Zhao *et al.*, "A Dynamic Gel with Reversible and Tunable Topological Networks and Performances," *Matter*, vol. 2, no. 2, pp. 390–403, Feb. 2020, doi: 10.1016/J.MATT.2019.10.020.

[8] L. Shi *et al.*, "Highly stretchable and transparent ionic conducting elastomers," *Nat. Commun.*, vol. 9, no. 1, 2018, doi: 10.1038/s41467-018-05165-w.

[9] C.-C. Kim, H.-H. Lee, K. H. Oh, and J.-Y. Sun, "Highly stretchable, transparent ionic touch panel," *Science (80-.).*, vol. 353, no. 6300, pp. 682–687, Aug. 2016, doi: 10.1126/science.aaf8810.

[10] W. Eom *et al.*, "Large-scale wet-spinning of highly electroconductive MXene fibers," *Nat. Commun. 2020 111*, vol. 11, no. 1, pp. 1–7, Jun. 2020, doi: 10.1038/s41467-020-16671-1.

[11] Z. Yang *et al.*, "On the cross-section of shaped fibers in the dry spinning process: Physical explanation by the geometric potential theory," *Results Phys.*, vol. 14, p. 102347, Sep. 2019, doi: 10.1016/J.RINP.2019.102347.

[12] J. Xue, T. Wu, Y. Dai, and Y. Xia, "Electrospinning and Electrospun Nanofibers: Methods, Materials, and Applications," *Chem. Rev.*, vol. 119, no. 8, p. 5298, Apr. 2019, doi: 10.1021/ACS.CHEMREV.8B00593.

[13] X. Wu *et al.*, "Microfluidic-spinning construction of black-phosphorus-hybrid microfibres for non-woven fabrics toward a high energy density flexible supercapacitor," *Nat. Commun. 2018 91*, vol. 9, no. 1, pp. 1–11, Nov. 2018, doi: 10.1038/s41467-018-06914-7.

[14] D. Ye, Y. Ding, Y. Duan, J. Su, Z. Yin, and Y. A. Huang, "Large-Scale Direct-Writing of Aligned Nanofibers for Flexible Electronics," *Small*, vol. 14, no. 21, p. 1703521, May 2018, doi: 10.1002/SMLL.201703521.

[15] M. Andersson *et al.*, "Biomimetic spinning of artificial spider silk from a chimeric minispidroin," *Nat. Chem. Biol. 2017 133*, vol. 13, no. 3, pp. 262–264, Jan. 2017, doi: 10.1038/nchembio.2269.

[16] X. Zhang *et al.*, "CRISPR/Cas9 Initiated Transgenic Silkworms as a Natural Spinner of Spider Silk," *Biomacromolecules*, vol. 20, no. 6, pp. 2252–2264, Jun. 2019, doi: 10.1021/ACS.BIOMAC.9B00193.

[17] C. Belbéoch, J. Lejeune, P. Vroman, and F. Salaün, "Silkworm and spider silk electrospinning: a review," *Environ. Chem. Lett. 2021 192*, vol. 19, no. 2, pp. 1737–1763, Jan. 2021, doi: 10.1007/S10311-020-01147-X.

[18] H. Bettahar, P. A. D. Harischandra, and Q. Zhou, "Robotic Threading from a Gel-like Substance Based on Impedance Control with Force Tracking," *IEEE Robot. Autom. Lett.*, vol. 7, no. 1, pp. 33–40, Jan. 2022, doi: 10.1109/LRA.2021.3116697.